Insulating behavior of magnetic spots in proton-bombarded graphite

K. Schindler,[1] N. García,[2,*] P. Esquinazi,[1,2,3,†] and H. Ohldag[4]
[1]*Division of Superconductivity and Magnetism, Institut für Experimentelle Physik II, Universität Leipzig, Linnéstraße 5, D-04103 Leipzig, Germany*
[2]*Laboratorio de Física de Sistemas Pequeños y Nanotecnología, Consejo Superior de Investigaciones Científicas, E-28006 Madrid, Spain*
[3]*CMAM, Universidad Autonoma de Madrid, Cantoblanco, E-28049 Madrid, Spain*
[4]*Stanford Synchrotron Radiation Laboratory, Stanford University, P.O. Box 20450, Menlo Park, California 94025, USA*
(Received 24 March 2008; revised manuscript received 3 July 2008; published 31 July 2008)

Kelvin probe force microscopy measurements on micrometer small magnetic spots produced by proton bombardment on bulk graphite reveal a charge transfer from the center of the spot to an external ring with potential variation on the order of 50 mV. The total charge in the spot is neutral. The results can be well understood in terms of practically unscreened potentials, an insulating property, although the nonbombarded, surrounding graphite region exhibits good conductance. Scanning transmission x-ray microscopy measurements on magnetic spots prepared on graphitic films reveal similar charge distribution. The insulating behavior is fundamental to understand the magnetism in graphite.

DOI: 10.1103/PhysRevB.78.045433 PACS number(s): 75.50.Dd, 68.37.−d, 75.30.Ds, 78.70.−g

I. INTRODUCTION

From the point of view of energy saving as well as for environmental reasons part of future studies in magnetism shall be related to the development of light, environmentally neutral magnetic materials with high electron-spin polarization. Recently published theoretical works indicate that carbon-based ferromagnetic materials without metallic elements are, in principle, ideal candidates because of the light weight of its main element as well as the high degree of spin polarization expected in some of their possible magnetic phases.[1–4] The magnetic order after proton bombardment of highly oriented pyrolytic graphite (HOPG) has recently been the subject of several studies. Evidence for this phenomenon has been obtained by direct magnetic moment measurements with a superconducting quantum interference device (SQUID)[5–7] as well as by x-ray magnetic circular dichroism (XMCD) on carbon films at room temperature.[8]

It has been recently shown[7] that irradiated micrometer small spots on pure graphite under relatively low proton fluences (~ 0.1 nC/μm^2) behave ferromagneticlike up to temperatures of ~ 400 K. Proton irradiation at MeV energies is a method that produces a ferromagnetic phase in a specific part of the sample interior only and therefore it does not allow for an easy characterization of the magnetic material, especially its electrical properties. However, this information is needed for theory to shed light on the mechanism that causes the ferromagnetic order in graphite. There are clear differences in the assumptions used by the theoretical models to obtain magnetic order in graphite,[4] either through the existence of defects[2,3,9] or hydrogen adatoms.[1,10] The knowledge whether ferromagnetic graphite behaves as a metal or as an insulator is therefore crucial. To provide an answer to this issue we have performed Kelvin probe force microscopy (KPFM) measurements on magnetic spots to study their screening characteristics. Complementing this method we also measured the x-ray absorption by a scanning transmission x-ray microscope (STXM) at the π- and σ-resonances. The STXM results presented in this work indicate that the used proton irradiation changes the π-electron band of graphite in such a way that the magnetic part shows insulating characteristics. This conclusion is supported independently by measurements of x-ray absorption on spots proved to be magnetic by XMCD measurements.

This paper is divided into four further sections. The experimental techniques and sample details are described in Sec. II. To introduce the reader to some details on irradiation damage and to clarify the evidence for magnetic order induced by proton irradiation in graphite, we discuss in Sec. III the SQUID data on HOPG samples with spots and before and after broad irradiation and the XMCD evidence. In this section we explain the possible reasons for the narrow window of irradiation parameters necessary to obtain a measurable ferromagnetic signal after irradiating graphite with monoenergetic protons. The KPFM and STXM results are presented and discussed in Sec. IV and the conclusions are drawn in Sec. V.

II. SAMPLES AND EXPERIMENTAL DETAILS

The magnetic spots on the HOPG sample were produced at 110 K by a proton microbeam of 2.25 MeV energy, perpendicular to the graphite planes.[7] Due to technical reasons the proton beam used had a slightly ellipsoidal shape with an average diameter of ~ 2 μm. Due to the lateral straggling the spots produced at the surface of the HOPG sample show ~ 4 μm average diameter each and are separated by ~ 5 μm [see atomic force microscopy (AFM) measurements in Fig. 1]. As reported in Ref. 7 robust magnetic signals appear when the defect concentration does not destroy the graphite structure and therefore low fluences are necessary. Particle induced x-ray emission (PIXE) measurements show a total of $\lesssim 0.5$ ppm metal impurity concentration in the used samples. SQUID measurements on this sample[7] provide a value of $m_s \simeq 2.5 \times 10^{-11}$ emu for the ferromagnetic moment at saturation per spot at room temperature, which can

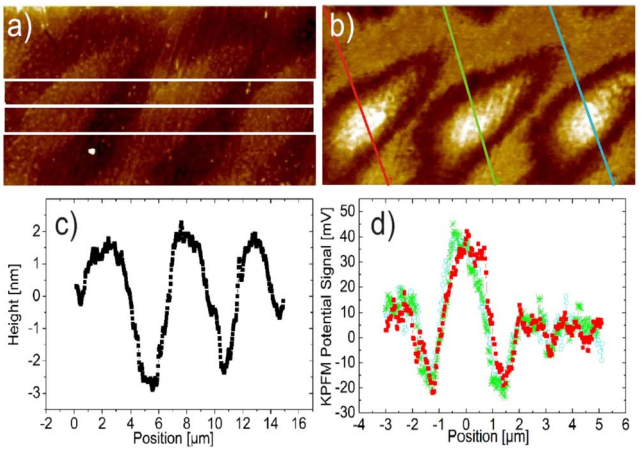

FIG. 1. (Color online) (a) AFM pictures showing three spots produced at a temperature of 110 K with a fluence of 0.124 nC/μm^2 and a proton current of 1 nA on HOPG. (b) KPFM pictures at the three spots. (c) AFM line scans across a horizontal line through the spots. (d) Potential variations obtained from the KPFM line scans for the three spots of (b). The color of the symbol corresponds to the same color line of the corresponding spot in (b).

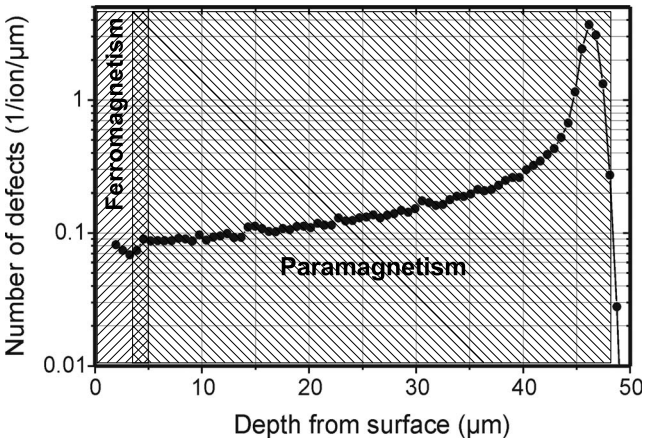

FIG. 2. (●): Number of defects per ion and per μm depth interval according to SRIM2003 Monte Carlo simulations (Ref. 13) for 2.25 MeV protons on HOPG. The data are obtained assuming a displacement energy of 35 eV for Frenkel pairs in HOPG. Following SQUID results obtained from HOPG samples irradiated with several thousands of spots at similar fluences as used for the spots discussed in this work (Ref. 7) the ferromagnetic region lies between the surface to ~5 μm depth. The rest of the irradiated sample depth shows a paramagnetic contribution. The overlapping region between ferromagnetism and paramagnetism depends on the fluence used. It is expected that it shifts to the right decreasing the fluence.

be translated into $10^{-3}\ldots10^{-2}\mu_B$ per C atom. Note that the SQUID measurements were done without direct sample handling using a single sample holder that can be used for SQUID as well as inside the irradiation chamber. In this way high accuracy and reproducibility is obtained.[6,7]

KPFM measurements are performed in two-pass mode; the first pass (tapping mode) gives the topography of the surface, while the second pass follows the track gotten in the first pass with an ac voltage applied between tip and sample to excite the cantilever oscillation. In this pass, a dc compensation voltage is applied by a feedback loop to compensate potential variations during scanning. The KPFM data were taken with ac amplitude of 3 V and 5 V, giving similar results. We used conductive, Pt-coated tips. The tip is set to vibrate at its resonant frequency of ≃70 kHz. All KPFM and AFM measurements were performed at ambient conditions. The potential signals at the spots are time independent within several months, in contrast to the intrinsic potential fluctuations observed in HOPG samples,[11] which show clear aging effects within half a month at ambient conditions.[12]

X-ray absorption measurements were performed with a scanning transmission x-ray microscope located at the elliptical polarizing undulator beamline 11.0.2 at the Advanced Light Source in Berkeley, California (USA). For these measurements a thin carbon film of ≈200 nm thickness was prepared by pulsed laser deposition (PLD) onto a self-supported, 200 nm-thick Si_3N_4 window. The carbon film was irradiated with the same proton beam as used for the HOPG sample to produce the spots. The STXM results discussed in this paper have been obtained on a spot produced with high fluence of 50 nC/μm^2. We note that the influence of the used proton fluence on the induced magnetic properties depends on the sample characteristics, i.e., whether the sample is a thin film of a bulk graphite, as well as its thermal contacts and the used proton current. The spot produced on the 200 nm-thick carbon film showed a similar ring structure as the spots produced at much lower fluence on the HOPG surface. For further details on the other characteristics of these spots produced on films, see Ref. 8.

III. SOME DETAILS ON THE MAGNETIC ORDER IN PROTON IRRADIATED GRAPHITE

The density of defects can be estimated from Monte Carlo simulations[13] taking into account the fluence (particles per area) irradiated and the atomic element(s) and density of the material. The reliability of this simulation program to obtain the defect concentration as a function of fluence and distance from the surface is well known for nuclear and material research scientists. For our case, graphite, the predictions of this program have been tested in irradiated spots.[14] Therefore, we expect that the error in the estimated density of defects and at the surface of our sample provided by this program is less than 20% because of the low annealing contribution in this part of the sample and the low fluence used.

Figure 2 shows the density of defects as a function of the sample depth from the surface for a graphite sample irradiated with protons of 2.25 MeV energy. At a fluence of 0.1 nC/μm^2 and according to the results shown in that figure we estimate a distance between defects in two dimensions of $\simeq 1.3 \pm 0.1$ nm. This distance decreases with the depth. Therefore, for the used irradiation fluence at the spots the graphite structure remains only in the first microns from the surface. According to the Monte Carlo results the protons leave a well-disordered graphite structure up to total amorphization already from a depth $\gtrsim 5$ μm up to the maximum at 46 μm (see Fig. 2). Clearly, due to the statistics of the

defect generation during irradiation we expect a smooth rather than a sharp interface between the magnetically ordered region and the disordered, paramagnetic one. That is the reason for the overlapping between regions depicted in Fig. 2. If we decrease the fluence we enhance the region where a graphite structure (with defects further apart) remains. Based on experimental results[7] we can assume that the defect density triggers magnetic order in the graphite structure. In this case by decreasing the fluence the total magnetic moment would also decrease proportional to the distance between defects to the square, at least, making it difficult to measure with a SQUID. On the other hand, if we increase the fluence the intermediate region between ferromagnetic and paramagnetic signals shifts to the sample surface, increasing the overall region with a well-disordered graphite structure and decreasing the overall ferromagnetic signal. This is the probable reason why a rather narrow window of fluence values is available to get a significant ferromagnetic SQUID signal. Note that this defect density estimation does not take into account defect recombination due to annealing effects during irradiation. Irradiation at low proton currents ($I \lesssim 1$ nA for microspots) is necessary to decrease the overall heating during irradiation. In the discussion above we did not take also the existence of hydrogen in the first micron from the surface[14] into account. This hydrogen may also play a role in triggering the ferromagnetic ordering[1–4,10] after it fixes to a carbon atom at or near a defect after irradiation.

A. SQUID measurements

Experimental evidence indicates that the microspots produced on pure graphite under relatively low proton fluences (~ 0.1 nC/μm^2) show typical signs for a magnetically ordered state up to a critical temperatures of ~ 400 K.[7] Typical *s*-type field dependence of the magnetic moment $m(H)$ at constant temperature plus irreversible behavior (ZFC-FC) of the remanence $[m(H=0)]$ after magnetizing the sample at low temperature suggest the existence of a magnetically ordered state at room temperature. Measurements with the SQUID of the magnetic moment of HOPG samples before and after irradiation with 25 600 spots and after taking out the first microns from the irradiated surface indicate the following:[7]

(a) There is a clear enhancement of the ferromagnetic signal after irradiation. Note that most of the virgin HOPG samples show a nonzero magnetic response.[15] Taking the difference of the $m(H)$ curves, i.e., after-minus before-irradiation, one gets typical ferromagneticlike curves with small coercive fields $H_c < 100$ Oe at 300 K.

(b) The difference between the $m(T)$ curves (after-minus before-irradiation) shows a paramagnetic Curie-type contribution ($m_P \sim 5/T$ μemu K) plus a ferromagneticlike signal that decreases linearly with T.

(c) After removing the first microns from the sample surface the measured magnetic moment $m(T,H)$ shows that $\sim 90\%$ of the ferromagnetic signals vanishes. Within experimental error the paramagnetic contribution produced by the irradiation remains in the rest of the sample.

Taking into account those results our work hypothesis is depicted in the shadow regions of Fig. 2 indicating that *at the used fluences* the main ferromagnetic part lies between the sample surface to a depth less than ~ 5 μm. The rest of the sample is highly disordered and contributes mainly to the measured paramagnetic signal.

Due to the micrometer small size of the spots one does not expect a large number of magnetic domains in the magnetic ordered part of the spot. Note that for similar spot size XMCD results indicate the existence of only a couple of domains in the irradiated spots on graphitic carbon films.[8] This appears to be also in agreement with the very small width of the hysteresis observed in HOPG samples with several thousands of spots. A standard method to check for the presence of ferromagnetic order is the Arrott plot[16] in which the third power of the magnetic moment (m) is plotted vs magnetic field (H) at fixed T. For this kind of plot and within the molecular-field model of ferromagnetism one expects to have a negative curvature below the Curie temperature and a transition to a positive curvature above T_C. If one plots m^2 vs the ratio H/m, following the molecular-field model, one expects isotherms with a slope that increases and an intercept in the x axis that tends to zero as the temperature approaches T_C from above. Especially measurements at low enough fields and near the critical temperature are the regions where one uses this kind of plot to determine Curie temperature and the ferromagnetic character of the measured signals.

This region in field and temperature is hardly accessible for our samples since all measurements suggest $T_C > 350$ K and the magnetic signal $m(H)$ produced by the irradiation and obtained from the difference between two curves has a relatively large error especially at low fields. Due to limited temperature range ($T < 390$ K) of the SQUID measurements (due to technical reasons) and the overall smallness of the signals at high temperatures, it is not possible to measure with high enough accuracy the behavior of $m(H, T \sim T_C)$. Nevertheless, we show in Fig. 3 $m(H)$ curves obtained from the sample with the spots shown in Fig. 1 at two temperatures and from a sample irradiated with a broad proton beam[6] where the remanent magnetic moment is not so small.

The sample irradiated with a broad beam shows at 300 K a typical ferromagnetic behavior within the Arrott plot (see Fig. 3). The samples with microspots have a small remanence as expected due to the micrometer small size of the magnetic spots. At first sight the two curves obtained for the sample with microspots show negative curvature [see Fig. 3(a)] and no definite conclusion on the curvature at low fields is possible. Using the same data we plot in Fig. 3(b) m^2 vs H/m. In this plot the peculiar behavior at low fields of the samples with the spots becomes evident. From this plot one would tend to ascribe this behavior to a paramagnetic or superparamagnetic state of the spots. However, we note that a positive curvature at low enough fields in the Arrott plot not necessarily indicates a nonferromagnetic paramagnetic character, especially in our samples. The first reason is that the region of validity of the Arrott-plot criterion shrinks dramatically when the ferromagnet has a distribution of exchange coupling strengths.[17] Since proton irradiation causes defects in both sublattices (A and B) of the graphite structure

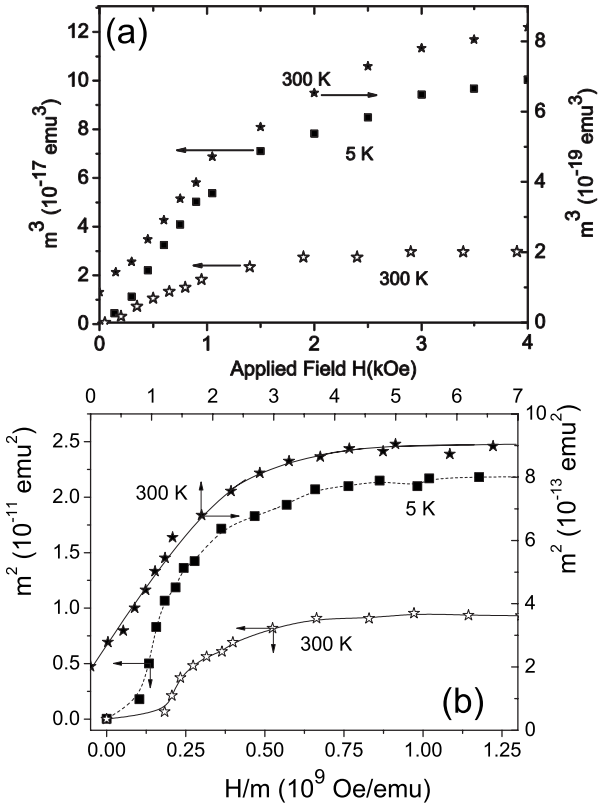

FIG. 3. (a) Magnetic moment to the third power vs applied field for two irradiated HOPG samples. The left *y* scale applies to the data from a sample irradiated with 25 600 spots at 5 K and 300 K (Ref. 7) and the right *y* axis to the data of a broad proton beam irradiated HOPG sample (Ref. 6). Note that the data points are taken from the difference between the data of the samples after-minus before-irradiation and for decreasing field only. (b) Magnetic moment to the second power vs applied field divided by the magnetic moment from the same data as in (a). The continuous lines are only a guide to the eyes.

and because of the expected antiferromagnetic coupling between defects of different sublattices,[2–4] the graphite samples should have competitive coupling strengths that certainly influence the slope of $m(H\rightarrow 0)$. This is an interesting subject that should be studied in future experiments. Second, the low and rather temperature independent fields at which the saturation of the magnetic moment occurs as well as its linear temperature dependence[7] speak against (super)paramagnetism.

B. Dichroism results

Proton irradiation in carbon leads to a spin polarized pi-band, according to the presented signals. The spin polarization of the pi-electrons leads to magnetic order as evidenced, for example, by the observation of magnetic domain patterns, the appearance of magnetic anisotropy, and the quantitative observation of a magnetic moment that cannot be explained by paramagnetism or any of its related phenomena at room temperature. X-ray absorption at the carbon *K*-edge only probes the electronic structure of the $2p$ final state, because only direct optical transition from $1s$ core-level electrons into $2p$ final states contribute to the absorption signal. The two main features in the carbon absorption spectra are labeled "π" and "σ" and refer to the two different types (symmetries) of p-orbitals that are possible. Due to the negligible core-hole interaction in carbon *K*-edge soft x-ray absorption, intermediate excited states are not observed, thus the line shape is only determined by the carbon π-states in the ground state. For an overview of the technique—and a detailed explanation why soft x-ray absorption is a probe of the electronic ground state—we refer to Ref. 18.

IV. ELECTRON FORCE MICROSCOPY AND SCANNING TRANSMISSION X-RAY MICROSCOPY RESULTS

A. Electron force microscopy results and their interpretation

Figure 1 shows the KPFM measurements on three spots of the HOPG sample. In the same figure we show the AFM and KPFM line scans. The AFM results indicate a slight modification of the topographic structure of graphite, i.e., a change in the topography height of $\lesssim 5$ nm in ~ 5 μm distance. The slightly ellipsoidal shape of the spots recognized by the KPFM pictures indicates that the spots were produced by a slightly out-of-focus proton microbeam. The KPFM measurements show a clear ring structure in the potential distribution around the centers of the spots, the hit positions of the microbeam. Similar ring structures were recently measured by XMCD, although those spots were produced on a thin carbon film. The XMCD measurements indicate that only the ring and not the center of the surroundings behaves magnetically ordered at room temperature and at an applied field of 600 Oe.[8]

Because the topography is adequately flat within the scan region of a spot [see Fig. 1(b)], the obtained signal can be considered as purely electrical, i.e., no interferences exist between the AFM and KPFM signals.

In what follows we shall interpret the potential distribution around the spot ($r=0$ denotes its center). The experimental voltage $V_e(r)$ can be written as the sum of two contributions,

$$V_e(r) = V_c(r) + W(r), \tag{1}$$

where $V_c(r)$ is the voltage variation due to a charge distribution within the spot and $W(r)$ is the work function variation divided by the electron charge. Assume $V_e(r)$ reflects the work function variation $W(r)$ without any charge displacement $V_c(r)$. Within this picture the corresponding physics is that the surface dipole, the origin of $W(r)$, is reduced in the center of the spot and gradually increases to a maximum at $r\sim 1.3$ μm from the spot center. At $r>1.3$ μm the magnitude of the dipole surface should gradually decrease to the level of HOPG at $r\gtrsim 1.8$ μm. Because the surface dipole is related to the surface spreading of the charge the results would indicate that the charge is retracted inside the sample surface at the center and is outspread at the external ring. Note that the resolution of our microscope is 20…50 nm$\ll$ spot radius. The results in Fig. 1(d) and Fig. 4 would imply a gradual change in W with r on the order of 50 meV. Due to the used low fluence and the small change of topology at the

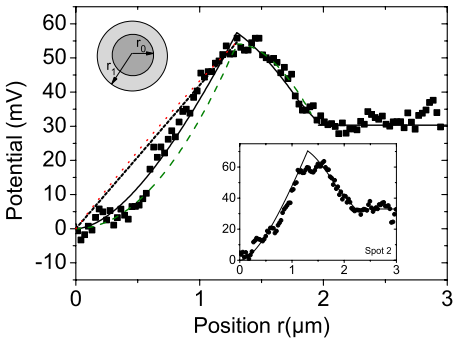

FIG. 4. (Color online) Potential variation through the spot #1 from its center. The dashed (green) line corresponds to the 3D unscreened potential according to Eq. (3) with parameter $\rho/2\epsilon = 64$ mV/μm^2; the continuous line corresponds to the 3D screened potential according to Eq. (4) with parameter $\rho/2\epsilon = 30$ mV/μm^2 and $\lambda = 6.7$ μm; the short dashed line (only for $r < 1.3$ μm) corresponds to the unscreened 2D potential according to Eq. (5) with parameter $(\rho h)/2\epsilon = 42$ mV/μm and the dotted (red) line to the 2D screened potential according to Eq. (6) with parameters $(\rho h)/2\epsilon = 48$ mV/μm and $\lambda = 5.3$ μm. The bottom inset shows the line scan data for the spot #2 and the continuous curve the fit following the 3D screened potential according to Eq. (4) with parameter $\rho/2\epsilon = 50$ mV/μm^2 and $\lambda = 3.6$ μm. The top left inset shows a sketch of the assumed cylindrical charge distribution from the top. The radii that are taken from the experimental data and included in the equations are $r_0 = 1.3$ μm and $r_1 = 1.8$ μm.

spot positions the graphite structure basically remains at the surface of the sample.[13] The maximum change in W expected from the displacement of one Bohr radius of a single electron per atom is $\lesssim 30$ eV. High quality graphite has an electron density of $n \lesssim 10^{-4}$ electrons per C atom. Therefore, the maximum change in $W(r)$ we would expect at the surface is $\lesssim 3$ meV, a value much smaller than the observed variations. Therefore, not only the gradual change but also the needed magnitude of variation of $W(r)$ appears unlikely.

There is an alternative explanation for the measured KPFM signals based on the potential created by a distribution of charges. Assume a density of positive charge ρ distributed homogeneously in a cylinder of height $h \sim 10$ μm—a distance equivalent to a depth where the defect density inside the sample remains practically constant[12,13]—and radius r_0 and the same density but negative between the radii r_0 and r_1 (see inset of Fig. 4). The expected potential due to this charge distribution can be written as

$$V_i(r) = \int_0^r v_i(r - r')d^i r', \tag{2}$$

where $v_i(r)$ represents the potential created by a punctual charge and the subindex i its type and dimensionality. For $i = 1$ we take the three-dimensional (3D) unscreened potential $1/r$, for $i = 2$ the 3D Thomas-Fermi screened potential $e^{-r/\lambda}/r$ with the screening length λ, for $i = 3$ the two-dimensional (2D) unscreened potential and for $i = 4$ the 2D Thomas-Fermi screened potential. These resulting V_i are

$$\begin{aligned} V_1(r) &= \rho r^2/4\epsilon, \quad 0 < r < r_0 \\ &= -V_1(r) + 2V_1(r_0)[1 + \ln(r/r_0)], \quad r_0 < r < r_1, \end{aligned} \tag{3}$$

$$\begin{aligned} V_2(r) &= \rho\lambda^2[1 - K_1(r/\lambda)r/\lambda]/(2\epsilon), \quad 0 < r < r_0 \\ &= -V_2(r) + 2V_2(r_0) + F(r,\lambda), \quad r_0 < r < r_1, \end{aligned} \tag{4}$$

where $K_1(x)$ is the modified Bessel function of second type order one and $F(r,\lambda)$ is a combination of products of modified Bessel and Struve functions.

In case we assume a quasi-2D charge distribution taking into account the anisotropy of the graphite structure, we have

$$V_3(r) = \frac{\rho h r}{2\epsilon}, \quad 0 < r < r_0, \tag{5}$$

$$V_4(r) = \rho\lambda h(1 - \exp - r/\lambda)/(2\epsilon), \quad 0 < r < r_0, \tag{6}$$

and a similar expression for the potential at $r_0 < r < r_1$ as in Eq. (3). For radius larger than r_1 the potential due to the positive and negative charge distributions decays within ~ 0.1 μm to the constant potential value of nonirradiated graphite. This potential $V(r_1 \leq r \lesssim r_1 + 0.15$ μm) can be written as a sum of the two potentials plus the screened potential due to the π-electrons of graphite.

Figure 4 shows the fits to the line scan potentials for two of the spots using different potentials $V_i(r)$. From the experimental data we obtain the two radii that enter in the model. The ratio between these radii agrees within experimental error to the expected ratio $r_1/r_0 = \sqrt{2}$ if we assume charge neutrality over the whole spot. A comparison between the data and the fits (see Fig. 4) indicates that unscreened 3D as well as screened 3D explain reasonably well the data, whereas the best fit is obtained for 3D screened potential $V_2(r)$ [Eq. (4)]. For the screening length we obtain values 3 μm$\lesssim \lambda \lesssim 7$ μm. As the spot size is on the order of ~ 2 μm the potential is practically unscreened implying that in the spot region there are no free π-electrons, i.e., the spot behaves as an insulator.

We note that for the number of π-electrons believed to exist in the nonirradiated region of graphite a $\lambda \sim 1$ nm has been estimated.[19,20] It is obvious that this value is far away from the one obtained at the spot. The other parameter we obtain from the fits is the charge density $\rho = 4 \pm 1.5$ C/m^3 (for $\epsilon = 10\epsilon_0$), which is equivalent to have ~ 25 electrons per μm^{-3}.

An increase in the proton fluence at the spot increases the maximum height at its center, e.g., from 100 nm to ~ 1 μm varying the fluence from 5 to 100 nC/μm^2. KPFM measurements done in those spots do not show any ring structure but a rather sharp increase in the potential difference where the second derivative of the height vs position has zeros. Due to the influence of the large topography change these data cannot be taken as signature of potential difference. Our results also indicate that magnetic force microscopy (MFM) measurements done in the past on irradiated spots[21] can be

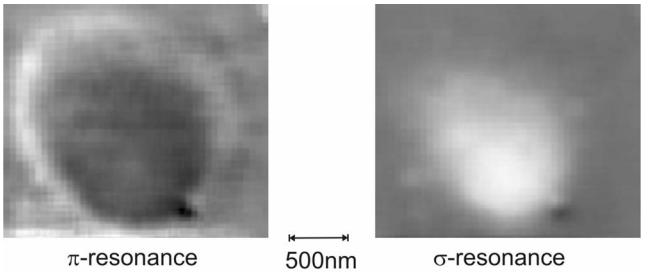

FIG. 5. (a) Transmitted x-ray intensity absorption at the π-resonance through a magnetic spot produced on a thin carbon film (sample A in Ref. 8). (b) The same but at the σ-resonance. The images are normalized using an image acquired at a photon energy below the absorption resonance to cancel out any contributions due to the topography. To eliminate any magnetic contrast from magnetic circular dichroism the images shown here are the result of averaging over two images acquired with opposite polarization of the x rays.

strongly influenced by electrostatic effects and care should be taken when the spot signals do not change with magnetic field. Finally we note that KPFM measurements obtain information with a penetration depth of microns. Therefore, we are exploring bulk properties.

B. Scanning transmission x-ray microscopy results

To further elaborate on the variation of the electronic structure and redistribution of charge caused by proton bombardment we present scanning STXM images of proton irradiated spots on graphite obtained at the carbon K absorption resonance. Recent XMCD measurements on these spots—obtained from the same sample—revealed that the outer area of these spots exhibit magnetic order at room temperature which origin is within the π-electron system.[8] To obtain the images, the energy of the incoming x rays is tuned such that core-level electrons are excited from the 1*s*-shell into empty 2*p*-states above the Fermi level. These 2*p*-states are split into levels with π- or σ-symmetry that can be addressed independently due to their energy separation of about 7 eV. Figure 5 shows STXM images that were acquired at the π and σ resonances. These resonances can be identified, for example, in the x-ray absorption spectra obtained from the same sample shown in Fig. 2 in Ref. 8.

The images in Fig. 5 show a spatial variation of the transmitted x-ray intensity due to changes in the 1*s*-2*p* x-ray absorption cross section. The outer area of the irradiated spot—the area which shows magnetic order[8]—exhibits a bright contrast at the π-resonance caused by a weaker π-absorption. This observation indicates that the number of occupied π-states in the ring is larger than in the rest of the sample.[22] The opposite behavior is observed in the central region of the spot that has been hit by the proton beam. This region shows a darker contrast and we can therefore conclude that the number of π-electrons is smaller in the central region. Altogether the STXM images show a redistribution of the occupied π-electron density from the center of the sample toward the magnetic ring. The observed change in the contrast at the π-resonance of the ring is about $\sim$10% compared to the background, which corresponds to an equal change of π-electrons per C atom. In the central region, however, it is a factor of 3 larger. This can be understood by taking into account that the central region also shows a contrast at the σ-resonance. Here, the proton irradiation leads to a change in the chemical bonding and structure of the graphite that causes an additional, local, redistribution of electron density from the π system to the σ system. The fact that we do not observe a magnetic response from this region[8] indicates that such a state is incompatible with magnetic order. Altogether the x-ray images corroborate the results obtained using the KPFM. They also suggest that proton irradiation leads to a retraction of π-electron charges at the center of the spot and a concentration at the external ring.

V. CONCLUSION

The KPFM as well as the x-ray absorption results indicate that there is a weak charge transfer within the spot and charge neutrality in the whole spot. The fact of having charge transfer and charge distribution implies that the magnetic material is an insulator and holds an average electric field of $\sim 10^3$ V/cm. Note that previous KPFM measurements on HOPG (Ref. 11) demonstrated potential fluctuations on the surface on the order of 10^4 electrons per μm^3 and holding fields up to 10^4 V/cm, a manifestation of the coexistence of conducting and insulating regions in graphite.

Note the fact that when a region of graphite is insulating does not mean that it is magnetic. The center of the irradiated spot has the largest defect amount, according to standard Monte Carlo simulations (Ref. 14), but it does not show any magnetic contrast, according to XMCD measurements.[8] A graphite flake inside a HOPG sample can have such a small defect density that the carrier density is extremely low. Therefore it has a different, much lower Fermi energy from the other, more defective flakes in the sample, and may behave as insulatinglike. Those flakes, though insulatinglike, do not show any XMCD contrast. In order words, insulating either because of perfect graphite or very disordered graphite or amorphous carbon does not imply magnetic order. The magnetism is found in irradiated, insulating spots with the charge distribution as described in the paper, that by the way, show charge neutrality.

Under proton bombardment there is a change in the vacancy density and therefore a change in the π-electron band making the material insulating, as the huge λ indicates. Because these results are obtained in magnetic spots, our results support the model of Ref. 4 that predicts an insulating-semiconducting magnetic state. In this model the disruption of the π-bonding opens a semiconducting gap at the Fermi level. The size of the energy gap as well as the magnetic coupling strength and therefore the critical temperature depend on the defect separation. Using SRIM2003[13] with full

damage cascades and 35 eV displacement energy, we obtain a vacancy density of 5×10^{20} cm^{-3} at the first microns from the surface, which means a distance between vacancies of 1.3 nm. According to Ref. 4 a 1.3 nm defect separation will lead to an energy gap of $\sim$100 meV in the graphene structure, clearly having an insulating behavior at room temperature.

ACKNOWLEDGMENTS

We gratefully acknowledge the collaboration and support of J. Barzola-Quiquia, D. Spemann, T. Butz, and M. Rothermel. This work was done with the support of the DFG under Grant No. ES 86/11, the Spanish CACyT and Ministerio de Educación y Ciencia and the EU project "Ferrocarbon."

*nicolas.garcia@fsp.csic.es
†esquin@physik.uni-leipzig.de

[1] E. J. Duplock, M. Scheffler, and P. J. D. Lindan, Phys. Rev. Lett. **92**, 225502 (2004).
[2] O. V. Yazyev and L. Helm, Phys. Rev. B **75**, 125408 (2007).
[3] H. Kumazaki and D. S. Hirashima, J. Phys. Soc. Jpn. **76**, 064713 (2007).
[4] L. Pisani, B. Montanari, and N. Harrison, New J. Phys. **10**, 033002 (2008).
[5] P. Esquinazi, D. Spemann, R. Höhne, A. Setzer, K.-H. Han, and T. Butz, Phys. Rev. Lett. **91**, 227201 (2003).
[6] J. Barzola-Quiquia, P. Esquinazi, M. Rothermel, D. Spemann, A. Setzer, and T. Butz, Nucl. Instrum. Methods Phys. Res. B **256**, 412 (2007).
[7] J. Barzola-Quiquia, P. Esquinazi, M. Rothermel, D. Spemann, T. Butz, and N. García, Phys. Rev. B **76**, 161403(R) (2007).
[8] H. Ohldag, T. Tyliszczak, R. Höhne, D. Spemann, P. Esquinazi, M. Ungureanu, and T. Butz, Phys. Rev. Lett. **98**, 187204 (2007).
[9] M. A. H. Vozmediano, M. P. Lopez-Sancho, T. Stauber, and F. Guinea, Phys. Rev. B **72**, 155121 (2005).
[10] K. Kusakabe and M. Maruyama, Phys. Rev. B **67**, 092406 (2003).
[11] Y. Lu, M. Muñoz, C. S. Steplecaru, C. Hao, M. Bai, N. García, K. Schindler, and P. Esquinazi, Phys. Rev. Lett. **97**, 076805 (2006).
[12] P. Esquinazi, *Handbook of Magnetism and Advanced Magnetic Materials* (Wiley, Chichester, UK, 2007), Vol. 4, pp. 2256–2281.
[13] J. F. Ziegler, *The Stopping and Range of Ions in Matter* (Pergamon, New York, 1977).
[14] P. Reichart *et al.*, Nucl. Instrum. Methods Phys. Res. B **249**, 286 (2006).
[15] P. Esquinazi, A. Setzer, R. Höhne, C. Semmelhack, Y. Kopelevich, D. Spemann, T. Butz, B. Kohlstrunk, and M. Lösche, Phys. Rev. B **66**, 024429 (2002).
[16] A. Arrott, Phys. Rev. **108**, 1394 (1957).
[17] I. Yeung, R. M. Roshko, and G. Williams, Phys. Rev. B **34**, 3456 (1986).
[18] J. Stoehr and H. C. Siegmann, *Magnetism: From Fundamentals to Nanoscale Dynamics* (Springer, Heidelberg, 2006), Chaps. 9 and 10, pp. 351–476.
[19] P. R. Visscher and L. M. Falicov, Phys. Rev. B **3**, 2541 (1971).
[20] F. Guinea, Phys. Rev. B **75**, 235433 (2007).
[21] K.-H. Han, D. Spemann, P. Esquinazi, R. Höhne, V. Riede, and T. Butz, Adv. Mater. (Weinheim, Ger.) **15**, 1719 (2003).
[22] Note that this does not indicate that the number of conduction electrons increases in the ring area. The π-states addressed here are well below E_F, hence do not contribute to the conductance.